

## Superfluid Dissipation in Rotating $^3\text{He-B}$

H. E. Hall,<sup>(a)</sup> P. L. Gammel, and J. D. Reppy

Laboratory of Atomic and Solid State Physics, and The Materials Science Center, Cornell University, Ithaca, New York 14853

(Received 17 January 1984)

Additional dissipation of oscillatory superflow has been observed in uniformly rotating  $^3\text{He-B}$ . The damping increases linearly with angular velocity and is interpreted in terms of vortex-induced mutual friction similar to that observed in superfluid  $^4\text{He}$ . In the nonrotating state the damping is amplitude dependent, and may contain a contribution from remanent vorticity.

PACS numbers: 67.50.Fi

The imposition of a sufficiently large rotational velocity on a superfluid system produces profound<sup>1</sup> modifications of the superfluid states. In the case of superfluid  $^4\text{He}$  the well-known quantized vortex lines appear in the rotating superfluid. Similar, but more complex, vortex structures are expected in  $^3\text{He-A}$  and  $-B$ , and recent NMR experiments<sup>2</sup> have already provided some evidence for their existence.

In this Letter we report the first observation of a rotation-induced dissipation for oscillatory superflow in  $^3\text{He-B}$ . This dissipation increases linearly with angular velocity. Similar dissipation in rotating  $^4\text{He}$  is attributed to mutual friction between quasiparticles and quantized vortex lines.<sup>3</sup> Using the same model of mutual friction as in  $^4\text{He}$ , we find the mutual friction coefficient in  $^3\text{He}$  to be roughly a factor of 2 larger.

While our most detailed experiments, reported here, have been in the  $B$  phase at 20 bars, we have observed similar effects in the  $A$  phase at 29 bars.

The flow cell is shown schematically in Fig. 1. The  $^3\text{He}$  sample is in the form of a thin slab, 2.5 cm wide, 9 cm long, and 0.1 mm thick, folded over on itself so that the end regions are separated only by a

thin, pressure-sensitive diaphragm. Displacement of the diaphragm is used to drive and detect flow in the slab. This geometry avoids the junctions from narrow flow channels to open volumes of helium that were present in earlier experiments.<sup>4</sup> The fill line enters at the center of the folded slab, so that it is at a pressure node of the oscillatory flow.

The diaphragm is 12- $\mu\text{m}$  Kapton,<sup>5</sup> and the outer walls of the cell are formed from 75- $\mu\text{m}$  Kapton sheet. The diaphragm is not tensioned at room temperature. It is simply held flat by two magnesium slabs cemented with Stycast<sup>6</sup> 1266 to the outer walls of the cell. Differential contraction brings the diaphragm into tension between 77 and 4 K. The separation of the cell walls is controlled by a temporary spacer of 75- $\mu\text{m}$  Kapton, which is pulled out at a late stage of construction. The Kapton sheets are sealed together with Stycast<sup>6</sup> 2850GT and the whole cell is encapsulated in the same material. A metal cage is embedded in this epoxy, for mechanical strength and thermal contact. The cell is mounted with the diaphragm horizontal, so that the experimental helium slab is largely perpendicular to the rotation axis of the cryostat.

Refrigeration is provided by a conventional PrNi<sub>5</sub> demagnetization cryostat, mounted on a platform capable of rotating at variable angular velocities of up to 0.75 rad/sec. The temperature of the helium reservoir was measured by a  $^3\text{He}$  melting-curve thermometer and a lanthanum-diluted cerium magnesium nitrate susceptibility thermometer. The thermal time constant of the cell was approximately 2 h when below  $T_c$ .

The diaphragm and the outer cell walls facing it are aluminized and the electrodes so formed are connected to a differential capacitance bridge. A dc bias is applied to the diaphragm. To detect fluid oscillations the bridge was driven at 395 Hz with a small, low-frequency amplitude modulation. In these experiments, our procedure was to set up flow oscillations at their resonant frequency. The

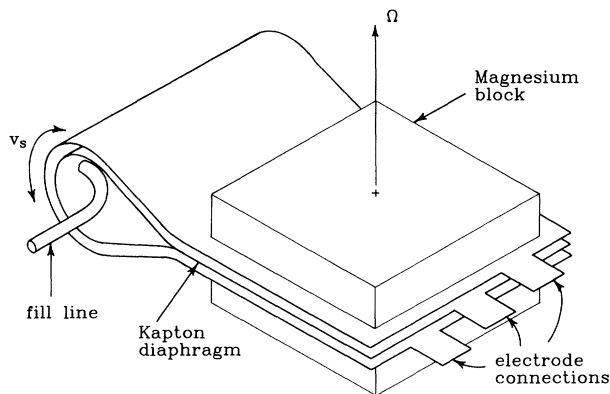


FIG. 1. Schematic view of the flow cell, without encapsulating epoxy.

low-frequency drive was then removed and the free decay of the oscillations observed.

An important calibration is provided by the observation of flow oscillations with the cell filled with liquid  $^4\text{He}$ . At 20 mK the  $^4\text{He}$  resonant frequency is  $\omega_0/2\pi = 6.61$  Hz and the  $Q$  is 5000. Since  $\omega_0^2$  is proportional to  $\rho_s/\rho^2$ , the  $^4\text{He}$  calibration enables us to deduce  $\rho_s$  in  $^3\text{He-B}$  from the oscillation frequency.

An additional calibration of the elastic properties of the diaphragm is provided by observation of the low-temperature vacuum resonance of the diaphragm. At a temperature of 1 K, a resonant frequency and  $Q$  of 1.86 kHz and 25 000 are observed. The static pressure sensitivity was determined by measuring the capacitance change due to the weight of the diaphragm as the mounting angle of the cell was varied continuously at 1.2 K in a test cryostat. Comparison of these results suggests a mean separation between the diaphragm and the outer walls of 100  $\mu\text{m}$ .

At temperatures above the  $^3\text{He}$  superfluid transition,  $T_c$ , the motion of the diaphragm is overdamped. The viscous relaxation time (proportional to  $1/T^2$ ) following a step in the bias voltage reaches a maximum value of approximately 250 sec at  $T_c$ .

Below the superfluid transition temperature the flow becomes oscillatory with a frequency of a few hertz. Figure 2 is a plot of the amplitude of the undriven superfluid oscillations in the nonrotating state. At high amplitude, for  $v_s > 0.1$  mm/sec, a region of linear damping (indicated by the straight line in Fig. 2) is observed. The  $Q$  for this nonrotat-

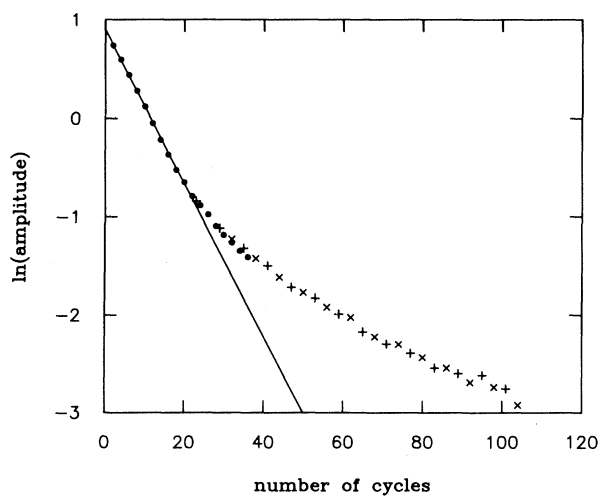


FIG. 2. The decay of superfluid oscillations in the nonrotating state at  $\omega_0/2\pi = 2.2$  Hz. Data from three decays with different starting conditions are shown. The line is a fit to the high-amplitude data points.

ing, high-amplitude regime is about 40. At lower amplitude another region of approximately linear damping is seen. In this case, the  $Q$  changes gradually from a value of 170 at  $\omega_0/2\pi = 2.2$  Hz to 90 at  $\omega_0/2\pi = 0.8$  Hz as  $T_c$  is approached.<sup>7</sup>

The dramatic effect of a superposed rotation with angular velocity  $\Omega$  is shown in Fig. 3. Even modest rotation rates cause a rapid quenching of superflow oscillations. At high rotation rates the oscillations decay in just a few cycles, and it is then only practical to make measurements in the high-amplitude linear region. At low rotation speeds measurements can also be made in the low-amplitude region. Typical results are shown in Fig. 4. Comparison of the two sets of points suggests that we use the empirical form

$$1/Q = [1/Q_1(v_s)] + [1/Q_2(\Omega)]. \quad (1)$$

The rotation-dependent term  $1/Q_2(\Omega)$  is seen to be roughly linear in  $\Omega$ . This linearity motivates an interpretation in terms of mutual friction due to quantized vortex lines, as in rotating superfluid  $^4\text{He}$ .<sup>3</sup> There is one feature of our experiment that is different from  $^4\text{He}$ , but similar to the Helsinki NMR experiments<sup>2</sup> on rotating  $^3\text{He}$ : Complete rotational equilibrium is attained rather rapidly, with a time constant of order 10 sec.

We choose to analyze our data in a manner analogous to that developed for the treatment of the attenuation of second sound in rotating  $^4\text{He}$ . Following the  $^4\text{He}$  treatment,<sup>3</sup> one obtains a mutual fric-

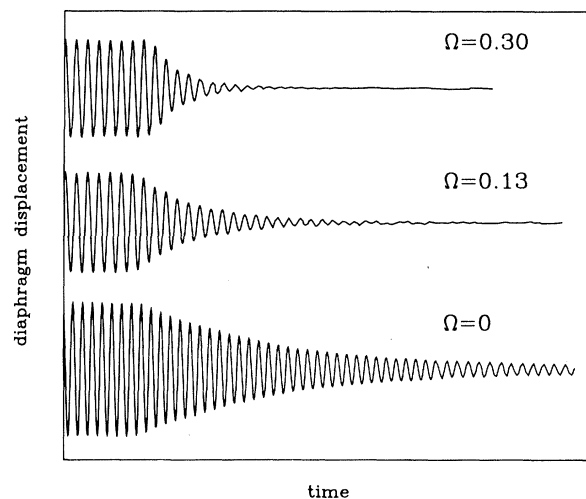


FIG. 3. The decay of superfluid oscillations at  $\omega_0/2\pi = 2.2$  Hz when the drive is removed (after six or seven cycles of oscillation) for various values of the angular velocity  $\Omega$ .

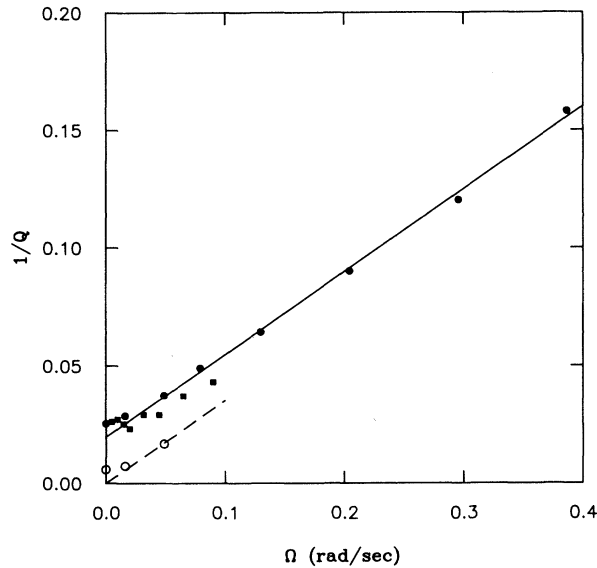


FIG. 4. The dependence of the damping on angular velocity  $\Omega$  for  $\omega_0/2\pi = 2.2$  Hz. Solid circles are  $v_s \sim 0.1$  mm/sec, open circles are  $v_s \sim 10 \mu\text{m/sec}$ . The solid line is a fit to all but the lowest two high-amplitude points. The broken line is a parallel line through the origin. The solid squares are high-amplitude data near  $\Omega = 0$ , taken at  $\omega_0/2\pi = 1.95$  Hz.

tion parameter  $B$  defined by

$$B = \omega_0 \frac{d(1/Q)}{d\Omega} \left( \frac{\rho}{\rho_n} \right). \quad (2)$$

Representative values for  $B\rho_n/\rho$  obtained in our experiment are listed in Table I. Equation (2) neglects the fact that not all of our helium slab is normal to the rotation axis. A correction for this condition will increase the listed values of  $B$  by about 20%. We also list in Table I values of  $\rho_s/\rho$  deduced from  $\omega_0$  and  $B(\rho_s/\rho)^{1/2}$ , which in  ${}^4\text{He}$  tends to a constant limit of 0.72 near  $T_\lambda$ .<sup>8</sup>

The recent third sound experiments of Kim and Glaberson<sup>9</sup> on rotating two-dimensional helium films also show a rotation-dependent dissipation. Their equation (3) may equivalently be written as

$$\vec{v}_l = -B(\rho_n/2\rho)\hat{z} \times \vec{v}_s + (1 - B'\rho_n/\rho)\vec{v}_s. \quad (3)$$

Equation (3) applied to their data gives  $B\rho_n/\rho \approx 3.4$  at the Kosterlitz-Thouless transition.

A small departure from linearity of  $Q_2^{-1}(\Omega)$  is shown in Fig. 4 for the high-amplitude data near  $\Omega = 0$ . Comparison with the fit to the high- $\Omega$  points suggests a residual vortex-line density in the nonrotating liquid of the order of that that would be

TABLE I. Rotational mutual friction parameters.

$\omega_0/2\pi$ (Hz)	$\rho_s/\rho$	$B(\rho_n/\rho)$	$B(\rho_s/\rho)^{1/2}$
1.1	0.0208	8.65	1.274
1.5	0.0386	5.19	1.061
1.9	0.0619	5.29	1.403
2.2	0.0830	4.85	1.524

produced by a rotation of  $10^{-2}$  rad/sec. This is about 30 lines/cm<sup>2</sup>. If we assume that  $Q$  at  $\Omega = 0$  is dominated by residual vorticity, then the  $Q$  at low amplitude in a sample of  ${}^3\text{He-B}$  containing no vortices could well be an order of magnitude higher, as expected on the basis of current theoretical ideas.<sup>7</sup>

The presence of vortex lines in undisturbed  ${}^4\text{He}$  has recently been investigated by Awschalom and Schwarz.<sup>10</sup> If the residual line density is controlled by the small dimension of our cell (100  $\mu\text{m}$ ) the line density is of factor of  $10^4$  less in  ${}^4\text{He-B}$  than  ${}^4\text{He}$ . This indicates that vortex-line creation and destruction may proceed with a much smaller free-energy threshold in  ${}^3\text{He-B}$  than for superfluid  ${}^4\text{He}$ .

We should like to thank N. D. Mermin for helpful comments and D. McQueeney and E. N. Smith for help with the figures. One of us (J.D.R.) would like to acknowledge the hospitality of the AT&T Bell Laboratories during the period when this manuscript was prepared. One of us (H.E.H.) would like to acknowledge the hospitality of the Low Temperature Group at Cornell University which made this experiment possible. This work has been supported by the National Science Foundation through the Cornell Materials Science Center under Contract No. 76-81083 AD2, Technical Report No. 5221. One of us (P.L.G.) is the recipient of an Andrew D. White Fellowship, 1980-1982.

<sup>(a)</sup>Permanent address: The Schuster Laboratory, Manchester University, M13 9PL, United Kingdom.

<sup>1</sup>D. N. Paulson, H. Kojima, and J. C. Wheatley, Phys. Rev. Lett. **32**, 1098 (1974).

<sup>2</sup>P. J. Hakonen, O. T. Ikkala, S. T. Islander, O. V. Lounasmaa, and G. E. Volovik, J. Low. Temp. Phys. **53**, 423 (1983); P. J. Hakonen, M. Kruiusius, M. M. Salomaa, J. T. Simola, Y. M. Bunkov, V. P. Mineev, and G. E. Volovik, Phys. Rev. Lett. **51**, 1362 (1983).

<sup>3</sup>H. E. Hall and W. F. Vinen, Proc. Roy. Soc. London, Ser. A **238**, 215 (1956).

<sup>4</sup>A. J. Dalm, D. S. Betts, D. F. Brewer, J. Hutchins,

and W. S. Truscott, Phys. Rev. Lett. **45**, 1411 (1980).

<sup>5</sup>E. I. du Pont de Nemours and Co., Chestnut Run, Wilmington, Delaware 19898.

<sup>6</sup>Emerson & Cumming, Inc., Canton, Massachusetts 02021.

<sup>7</sup>A discussion of the  $Q$ 's in  $^3\text{He}$  flow experiments may be found in H. E. Hall and J. R. Hook, in "Progress in Low Temperature Physics," edited by D. F. Brewer (North-Holland, Amsterdam, to be published), Vol. IX. For the boundary conditions of the present experimental cell, the damping due to second viscosity is

$$1/Q = 1.26\rho_n^2\xi_3\omega_0/M\omega_0^2d.$$

Here  $\xi_3$  is second viscosity,  $M$  is the mass per unit area of the diaphragm,  $\omega_0$  is the vacuum resonance frequency, and  $d$  is the thickness of the slab. Both this and ordinary viscosity predict  $Q \geq 1000$ . Our low values are very much as in the experiments at Sussex (Ref. 4).

<sup>8</sup>P. Mathieu, A. Serra, and Y. Simon, Phys. Rev. B **14**, 3753 (1976).

<sup>9</sup>M. Kim and W. I. Glaberson, Phys. Rev. Lett. **52**, 53 (1984).

<sup>10</sup>D. D. Awschalom and K. W. Schwarz, Phys. Rev. Lett. **52**, 49 (1984).